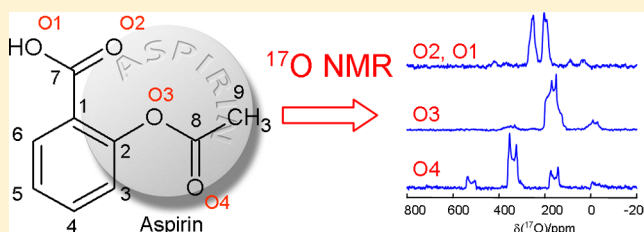


Solid-State ^{17}O NMR of Pharmaceutical Compounds: Salicylic Acid and AspirinXianqi Kong,[†] Melissa Shan,[†] Victor Terskikh,^{†,‡} Ivan Hung,[§] Zhehong Gan,[§] and Gang Wu^{*,†}[†]Department of Chemistry, Queen's University, 90 Bader Lane, Kingston, Ontario, K7L 3N6, Canada[‡]National Research Council Canada, 100 Sussex Drive, Ottawa, Ontario, K1A 0R6, Canada[§]Center of Interdisciplinary Magnetic Resonance, National High Magnetic Field Laboratory, 1800 East Paul Dirac Drive, Tallahassee, Florida 32310, United States

S Supporting Information

ABSTRACT: We report solid-state NMR characterization of the ^{17}O quadrupole coupling (QC) and chemical shift (CS) tensors in five site-specifically ^{17}O -labeled samples of salicylic acid and *o*-acetylsalicylic acid (Aspirin). High-quality ^{17}O NMR spectra were obtained for these important pharmaceutical compounds under both static and magic angle spinning (MAS) conditions at two magnetic fields, 14.0 and 21.1 T. A total of 14 ^{17}O QC and CS tensors were experimentally determined for the seven oxygen sites in salicylic acid and

Aspirin. Although both salicylic acid and Aspirin form hydrogen bonded cyclic dimers in the solid state, we found that the potential curves for the concerted double proton transfer in these two compounds are significantly different. In particular, while the double-well potential curve in Aspirin is nearly symmetrical, it is highly asymmetrical in salicylic acid. This difference results in quite different temperature dependencies in ^{17}O MAS spectra of the two compounds. A careful analysis of variable-temperature ^{17}O MAS NMR spectra of Aspirin allowed us to obtain the energy asymmetry (ΔE) of the double-well potential, $\Delta E = 3.0 \pm 0.5$ kJ/mol. We were also able to determine a lower limit of ΔE for salicylic acid, $\Delta E > 10$ kJ/mol. These asymmetrical features in potential energy curves were confirmed by plane-wave DFT computations, which yielded $\Delta E = 3.7$ and 17.8 kJ/mol for Aspirin and salicylic acid, respectively. To complement the solid-state ^{17}O NMR data, we also obtained solid-state ^1H and ^{13}C NMR spectra for salicylic acid and Aspirin. Using experimental NMR parameters obtained for all magnetic nuclei present in salicylic acid and Aspirin, we found that plane-wave DFT computations can produce highly accurate NMR parameters in well-defined crystalline organic compounds.



1. INTRODUCTION

There has been an increasing interest in recent years to extend the realm of solid-state ^{17}O ($I = 5/2$) NMR spectroscopy to studies of a wide range of molecular systems from inorganic materials^{1,2} to organic and biological molecules.^{3–5} Compared to the routine use of ^1H , ^{13}C , ^{15}N , and ^{31}P NMR techniques that rely on detection of spin-1/2 nuclei, quadrupolar ^{17}O NMR is far less common, despite the importance and ubiquity of oxygen-containing functional groups in chemical compounds. Since the only NMR-active oxygen isotope, ^{17}O , has an exceedingly low natural abundance of 0.037%, a prerequisite of ^{17}O NMR studies of large biomolecules is to introduce the ^{17}O isotope into the functional group of interest. Another challenge in ^{17}O NMR is to deal with the intrinsic sensitivity and resolution limitations of detecting a half-integer quadrupolar nucleus. In particular, one can usually detect only the central transition (CT) in ^{17}O NMR studies of solids. For a spin-5/2 nucleus such as ^{17}O , the maximum CT intensity generated by a single selective RF pulse is only 8.6% of the total signal intensity, thus giving rise to a low intrinsic sensitivity in CT-based experiments. Furthermore, the second-order quadrupolar broadening of the CT cannot be completely removed

by the magic-angle spinning (MAS) technique and, as such, imposes a limitation on the resolving power of this most commonly used solid-state ^{17}O NMR technique. For liquid samples, molecular tumbling often causes rapid quadrupole relaxation that leads to rather broad lines in ^{17}O NMR spectra. These limitations have so far set some boundaries for chemical and biological applications of ^{17}O NMR. A general approach to overcome these difficulties is to perform ^{17}O NMR experiments on highly ^{17}O -enriched samples at the highest magnetic field available. For example, we demonstrated that it is possible to obtain ^{17}O CT NMR spectra for large protein–ligand complexes (e.g., 80–240 kDa) in both solid and solution states at 21.1 T.^{6–8} Another new emerging trend is to utilize ^{17}O NMR to obtain information about molecular dynamics in organic solids.⁹ Recently, Michaelis et al.¹⁰ and Blanc et al.¹¹ showed that dynamic nuclear polarization (DNP) can be used to drastically enhance the sensitivity of ^{17}O NMR spectroscopy. Although these two studies were carried out at moderate

Received: May 27, 2013

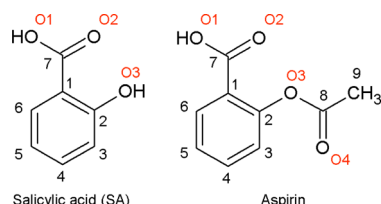
Revised: July 21, 2013

Published: July 23, 2013

magnetic fields, it is certainly not impossible to overcome the technological hurdles in the near future so that DNP can be performed at ultrahigh magnetic fields. As a result of these new developments, it has become quite clear that the traditional difficulties hampering the development of ^{17}O NMR spectroscopy are gradually disappearing.

In the present work, we report ^{17}O -isotope labeling and solid-state ^{17}O NMR studies of two important pharmaceutical compounds: salicylic acid (SA) and *o*-acetylsalicylic acid (Aspirin); see Scheme 1. Between these two molecules, there

Scheme 1. Molecular Structures of SA and Aspirin and the Atomic Numbering Used in This Study



are a total of seven oxygen sites that can be used as ^{17}O NMR probes. The medicinal use of SA can be traced back to the ancient Greek physician Hippocrates who prescribed extracts from willow bark for patients to relieve pain and fever.¹² SA is now used in many modern drugs and health products. Aspirin is perhaps the best known “wonder drug”. According to the Aspirin Foundation (<http://www.aspirin-foundation.com/>), approximately 35 000 t of Aspirin are produced and consumed annually worldwide, making it the most widely used drug of all times. In recent years, over 2000 scientific papers are published annually on the topic of Aspirin.¹³

The crystal structure of SA was first determined by Cochran in 1953.¹⁴ Later, Sundaralingam and Jesen¹⁵ reported a further refinement of the X-ray structure and Bacon and Jude¹⁶ reported a crystal structure of SA determined by neutron diffraction. The crystal structure of Aspirin was first established in 1964.¹⁷ Subsequently, higher quality X-ray and neutron structures were also reported.^{18–20} For many decades, it was believed that crystalline Aspirin exists in only one polymorph (also known as form-I). In 2005, Zaworotko and co-workers²¹ reported the preparation and crystal structure of a new Aspirin

polymorph (form-II). Although there was debate about the initial data interpretation, it seems that the existence of Aspirin form-II polymorph has now been firmly established.^{22–24} Similar to many carboxylic acids, SA and Aspirin molecules form centrosymmetric hydrogen bonded dimers in the crystal lattice, as illustrated in Figure 1. In each dimer, the O...O separation is approximately 2.6 Å, corresponding to a medium-strength hydrogen bond. A particularly interesting phenomenon in this kind of carboxylic acid dimers is concerned with the proton dynamics involving a concerted double proton transfer across two symmetry-related hydrogen bonds. In general, this proton transfer process is associated with a double-well potential. As the proton movement between the two potential minima is often less than 0.6 Å, translational quantum tunneling may become important. This is particularly true when the double-well potential is nearly symmetrical. In the solid state, however, crystal packing often introduces an energy asymmetry between the two minima of the potential curve. While there have been intense investigations of proton dynamics in carboxylic acid dimers in which many spectroscopic techniques including solid-state ^1H and ^{13}C NMR were employed,²⁵ solid-state ^{17}O NMR has not been utilized in this area, except for two brief reports on the solid-state ^{17}O NMR spectra of benzoic acid.^{26,27} For SA and Aspirin, surprisingly, there were only very limited solid-state NMR data available in the literature. These include early solid-state ^{13}C NMR^{28,29} and ^2H NMR³⁰ studies of Aspirin. Also related to the present work are early ^2H and ^{17}O nuclear quadrupole resonance (NQR) studies of SA and Aspirin.^{31–33}

The present work was carried out with the following objectives in mind. First, we investigate the most efficient synthetic routes for introducing ^{17}O isotope into each of the oxygen sites in SA and Aspirin. Second, we fully characterize the ^{17}O QC and CS tensors for all oxygen sites in these two compounds. Third, we examine the effect of proton dynamics on the ^{17}O NMR tensor parameters. Fourth, we evaluate the accuracy of plane-wave DFT computation by simultaneously examining solid-state NMR parameters for *all* magnetic nuclei (^1H , ^{13}C , and ^{17}O) present in SA and Aspirin. Finally, solid-state NMR has become increasingly indispensable for characterization of active pharmaceutical ingredients (APIs),^{34,35} and recent advances in this area include applications of high-

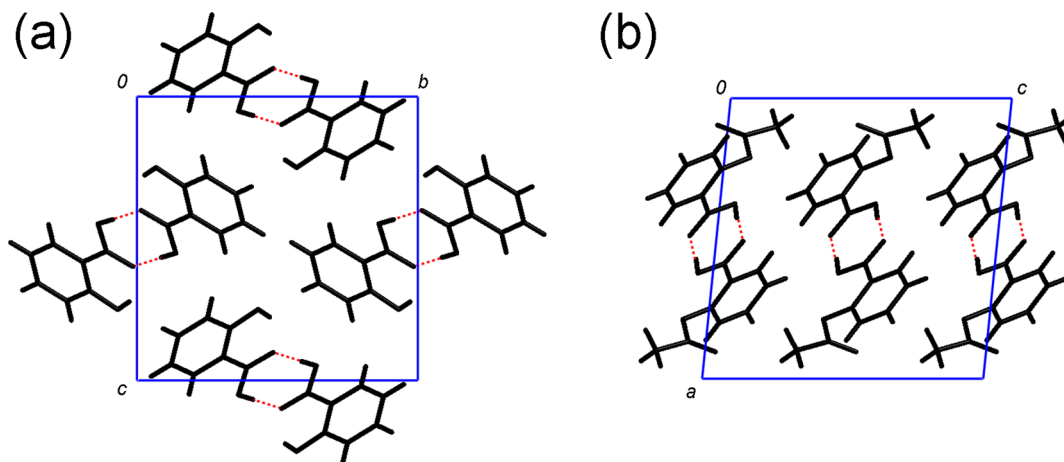


Figure 1. Hydrogen-bonded dimer formation in the crystal lattice of (a) SA (monoclinic, space group $P2_1/c$, $a = 4.889$, $b = 11.241$, $c = 11.335$ Å, $\beta = 91.919^\circ$, cell volume = 622.631 Å³) and (b) Aspirin (monoclinic, space group $P2_1/c$, $a = 11.278$, $b = 6.552$, $c = 11.274$ Å, $\beta = 95.84^\circ$, cell volume = 828.696 Å³).

resolution solid-state ^1H NMR^{36–38} and studies of quadrupolar nuclei such as ^{14}N ($I = 1$),^{39,40} ^{23}Na ($I = 3/2$),⁴¹ and $^{35/37}\text{Cl}$ ($I = 3/2$).^{42,43} In this broad context, we explore in this work the potential of adding ^{17}O as a new NMR probe for studying pharmaceutical compounds.

2. EXPERIMENTAL DETAILS

2.1. Synthesis. Preparation of $[1,2-^{17}\text{O}_2]\text{Salicylic Acid}$. In an NMR tube (5 mm o.d.) were mixed salicylic acid (413 mg), 40% ^{17}O -enriched water (64 mg, purchased from CortecNet), 1,4-dioxane (0.5 mL), and 4 M HCl in 1,4-dioxane (0.5 mL). The tube was capped and heated in an oil bath at $86 \pm 3^\circ\text{C}$ for 30 h. The ^{17}O NMR spectra indicated that the oxygen isotope exchange was complete. The content of the tube was transferred into a flask, and the solvent was removed on a rotary evaporator. The residual material was dried under a vacuum, giving the title compound as a white solid (394 mg). The ^{17}O enrichment level in the compound was estimated to be approximately 20% by solution ^{17}O NMR (67.7 MHz, $\delta = 266.0$ ppm with respect to the signal of liquid water).

Preparation of $[3-^{17}\text{O}]\text{Salicylic Acid}$. In a dry, nitrogen-flushed pressure tube were placed 8-hydroxyquinoline (180 mg), copper(I) iodide (140 mg), 2-iodobenzoic acid (1.5 g), and potassium *tert*-butoxide (2.68 g). The tube was capped with a rubber septum. To the mixture were added, via syringe, *tert*-butanol (3 mL) and anhydrous DMSO (6 mL). A flow of N_2 was passed through the mixture for 2 min, followed by addition of 20% ^{17}O -enriched water (660 mg). After replacing the septum with a pressure cap, the mixture was stirred in an oil bath at $100 \pm 5^\circ\text{C}$ for 44 h. After cooling down to room temperature, the mixture was acidified with concentrated HCl (1 mL) to pH 3–4. Insoluble materials were removed by filtration. The filtrate was extracted with ethyl acetate (6×20 mL). The organic extract was washed with 0.1 M HCl (15 mL), water (15 mL), and brine (2×10 mL) and then decolorized with active carbon. After solvent removal with a rotary evaporator, the solid residue was recrystallized from water (10 mL), giving the title compound as a white crystalline solid (415 mg, yield 50%): The liquid-state ^{17}O NMR spectrum (67.7 MHz, $\delta = 83.2$ ppm with respect to the signal of liquid water) suggests the compound has an ^{17}O -enrichment level of 20%.

Preparation of $[1,2-^{17}\text{O}_2]\text{Aspirin}$. $[1,2-^{17}\text{O}_2]\text{Salicylic acid}$ (278 mg) was dissolved in anhydrous THF (10 mL) and pyridine (0.6 mL). The flask was capped with a rubber septum, followed by addition of acetyl chloride (0.6 mL). The mixture was stirred at room temperature for 20 min. After solvent removal with a rotary evaporator at 20°C , the residual material was treated with cold water (15 mL) and the mixture was stirred in an ice–water bath for 2 h. The solid material was collected by filtration, washed with cold water (3×3 mL), and dried under a vacuum, giving the title compound as a white powder (204 mg): ^{17}O NMR (67.7 MHz, $\delta = 258.8$ ppm with respect to the signal of liquid water). The ^{17}O enrichment level in the compound is the same as in $[1,2-^{17}\text{O}_2]\text{salicylic acid}$, ca. 20%.

Preparation of $[3-^{17}\text{O}]\text{Aspirin}$. $[3-^{17}\text{O}]\text{Salicylic acid}$ (280 mg) was dissolved in pyridine (0.8 mL) in a flask capped with a rubber septum and cooled in an ice–water bath. To the cold solution was added acetyl chloride (0.25 mL), and the mixture was kept in the ice–water bath (with occasional shaking) for 50 min. After addition of anhydrous THF (1 mL), the mixture was kept in the ice–water bath for another 25 min, followed by

addition of cold water (10 mL). The cold mixture was then acidified with a concentrated HCl(aq) solution to pH 1–2 (approximately 0.45 mL of HCl) and was stirred in the ice–water bath for 1 h. Solid material was collected, washed with cold water (3×3 mL), and dried under a vacuum, producing the title compound as a white solid (230 mg): ^{17}O NMR (67.7 MHz, $\delta = 196.6$ ppm with respect to the signal of liquid water). The ^{17}O enrichment level in the compound is the same as that in $[3-^{17}\text{O}]\text{salicylic acid}$, ca. 20%.

Preparation of $[4-^{17}\text{O}]\text{Aspirin}$. In a 25 mL round-bottom flask equipped with a rubber septum was first added acetyl chloride (0.36 mL) and then 40% ^{17}O -enriched water (90 μL) via a syringe. A needle was inserted into the flask for gas release. The mixture was kept at room temperature for 10 min with occasional shaking. Anhydrous THF (3 mL) was added into the flask through a syringe, and the mixture was kept at room temperature for 10 min. To the solution was added thionyl chloride (0.36 mL), and the mixture was heated briefly with a hot gun to lukewarm and then left at room temperature for 1 h. The flask was cooled in an ice–water bath for 10 min, followed by addition of salicylic acid (420 mg) in anhydrous pyridine (1 mL) via a syringe. The mixture was kept in the ice–water bath for 1 h, and then, the solvent was removed on a rotary evaporator at 20°C (for about 20 min.). To the residual material was added cold water (15 mL). The mixture was cooled in an ice–water bath and acidified with a concentrated HCl(aq) solution to pH 1–2. The mixture was stirred in the cold bath for 20 min. The solid material was collected, washed with cold water (3×3 mL), and dried under a vacuum, giving the title compound as a white powder: ^{17}O NMR (67.7 MHz, $\delta = 368.0$ ppm with respect to the signal of liquid water). The ^{17}O enrichment level in the compound is ca. 40%.

2.2. Solid-State ^{17}O NMR. Room-temperature solid-state ^{17}O NMR spectra were obtained at 14.0 T (Queen's University, Kingston, Ontario, Canada) and 21.1 T (National Ultrahigh-Field NMR Facility for Solids, Ottawa, Ontario, Canada). At 14.0 T, the MAS experiments were performed on a Bruker 4 mm H/X MAS probe with a sample spinning of 14.5 kHz. ^{17}O MAS NMR spectra at 21.1 T were acquired using a 3.2 mm H/X MAS Bruker probe with a sample spinning frequency of 22 kHz. It is important to point out that, under this MAS spinning speed, the actual temperature of the sample was determined to be about 20 K higher than the room temperature, 298 K, due to frictional heating of the sample. A rotor-synchronized 90° -delay- 180° -echo pulse sequence was used with a CT-selective 90° pulse length of 3 μs . Typically, relaxation delays of 2–5 s were found sufficient for most samples, and the number of scans varied from 2048 to 4096. The proton decoupling was normally not used when acquiring ^{17}O MAS spectra at 21.1 T, because the ^1H – ^{17}O dipolar coupling is effectively suppressed by fast MAS. At 21.1 T, static ^{17}O NMR spectra were acquired with a home-built 5 mm H/X solenoid probe using a 90° -delay- 90° -echo pulse sequence to avoid powder line shape distortions. To minimize the unwanted ^{17}O background signals, the powder samples were packed in 5 mm o.d. Teflon tubes (Norell). The high power proton decoupling (ca. 70 kHz) was used to acquire all static spectra. The CT-selective $\pi/2$ pulse length was 2 μs , and the echo delay was 50 μs . Typically, 4096 scans were accumulated for each spectrum using a relaxation delay of 2–5 s. ^1H MAS NMR spectra were acquired at 21.1 T using a 1.3 mm H/X MAS Bruker probe with a sample spinning of 62.5 kHz. A rotor-synchronized 90° -delay- 90° -echo pulse sequence was used with a ^1H 90° pulse length of 2 μs . The

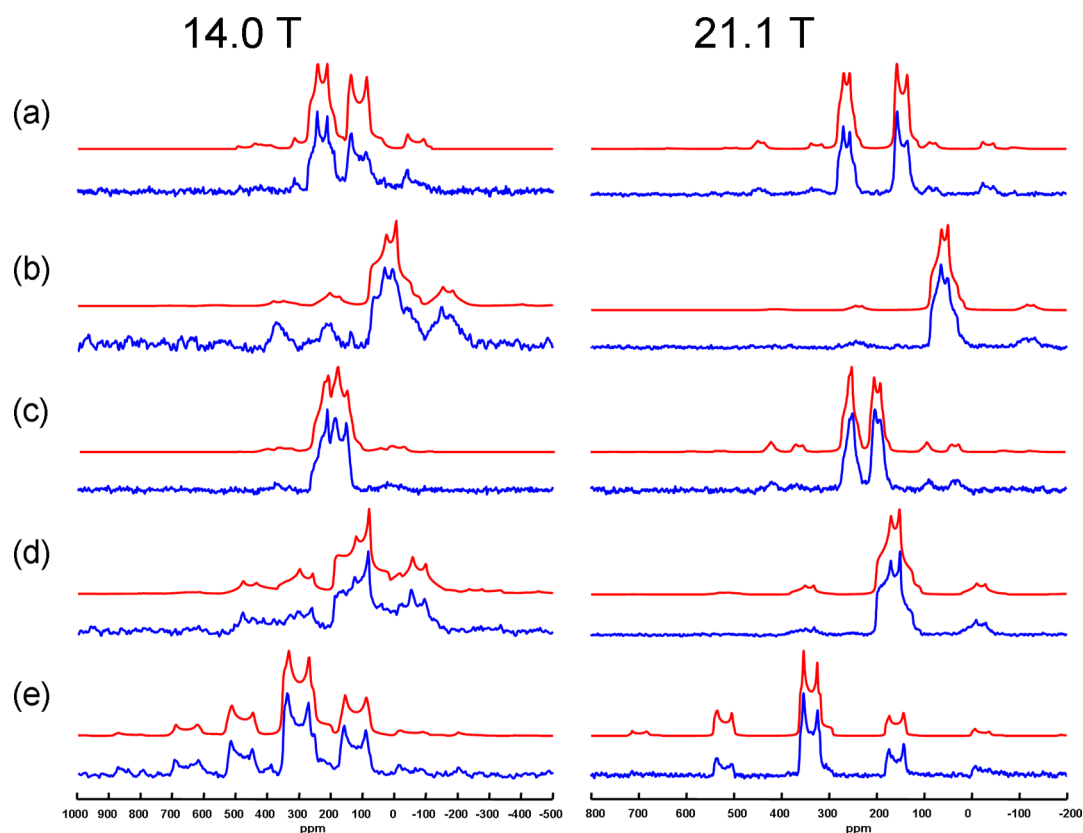


Figure 2. Experimental (lower trace) and simulated (upper trace) ^{17}O MAS NMR spectra at two magnetic fields for (a) $[1,2-^{17}\text{O}_2]\text{SA}$, (b) $[3-^{17}\text{O}]\text{SA}$, (c) $[1,2-^{17}\text{O}_2]\text{Aspirin}$, (d) $[3-^{17}\text{O}]\text{Aspirin}$, and (e) $[4-^{17}\text{O}]\text{Aspirin}$. The sample spinning frequency was 14.5 and 22.0 kHz for spectra collected at 14.0 and 21.1 T, respectively. All spectra were recorded at room temperature. The recycle delay (RD) and number of scans (NS) for spectra collected at 14.0 and 21.1 T are given below. In part a, RD = 1 s, NS = 15250; RD = 5 s, NS = 1024. In part b, RD = 2 s, NS = 19746; RD = 5 s, NS = 2048. In part c, RD = 2 s, NS = 10628; RD = 5 s, NS = 2048. In part d, RD = 5 s, NS = 9899; RD = 5 s, NS = 7168. In part e, RD = 1 s, NS = 11877; RD = 5 s, NS = 2048.

residual proton background signal was further removed by recording a background spectrum using a rotor containing NaCl(s) and then subtracting it out from the actual spectrum. The relaxation delay was 60 s, and the number of scans was either 64 or 128. Solid-state ^{13}C NMR spectra were recorded at 14.0 T under the cross-polarization (CP), MAS, and high-power ^1H decoupling conditions. Variable-temperature (VT) ^{17}O MAS NMR spectra were obtained at 21.1 T (National High Magnetic Field Laboratory, Tallahassee, FL, USA) with a 900 MHz Bruker Avance console and a 3.2 mm home-built MAS H/X transmission line probe. Sample temperatures under the 20 kHz MAS condition were calibrated using solid $\text{Pb}(\text{NO}_3)_2$, and the actual temperature range of the VT MAS probe was 360–146 K. Spectral analyses were performed with the DMfit software.⁴⁴ All ^{17}O chemical shifts were referenced to the signal of a liquid water sample, and ^1H and ^{13}C chemical shifts were referenced to the signals of TMS.

2.3. Plane-Wave DFT Calculations. All plane-wave DFT calculations were performed with the CASTEP software⁴⁵ and the Materials Studio 4.4 program (Accelrys) running on a Linux server with two 2.66 GHz processing cores and 8 GB of RAM. Perdew, Burke, and Ernzerhof (PBE) functionals were used with a plane wave basis set cutoff of 610 eV and a $3 \times 1 \times 2$ Monkhorst–Pack k -space grid. The most recent crystal structures of SA (CCDC code: 871047)⁴⁶ and Aspirin (CCDC code: 610952)²² were used as initial structures, and then, a full optimization was performed for each structure while

keeping the unit cell parameters at their experimental values. Some key bond lengths from various X-ray, neutron, and CASTEP-optimized crystal structures of SA and Aspirin are compared in the Supporting Information. In general, the fully CASTEP-optimized structures have bond lengths and angles that are within the experimental uncertainties of the neutron diffraction structures. Magnetic shielding tensors and electric field gradient (EFG) tensors were then calculated for all nuclei with the gauge-including projector augmented wave (GIPAW)^{47,48} and PAW methods as implemented in CASTEP. Calculated magnetic shielding values (σ_{calc}) were converted to chemical shifts (δ_{calc}) using the expression $\delta_{\text{calc}} = \sigma_{\text{ref}} - \sigma_{\text{calc}}$ with the values for σ_{ref} previously reported as being 259.0, 175.1, and 31.0 ppm for ^{17}O , ^{13}C , and ^1H nuclei, respectively.⁴⁹ In this study, σ_{ref} was not used as an adjustable parameter in the comparison between computed and experimental chemical shifts.

3. RESULTS AND DISCUSSION

3.1. Extraction of ^{17}O NMR Tensor Parameters. Figure 2 shows the ^{17}O MAS NMR spectra obtained for the five compounds of site-specifically ^{17}O -labeled SA and Aspirin at 14.0 and 21.1 T. One can see clearly that the spectra obtained at 21.1 T are generally of higher quality than those obtained at 14.0 T. We were able to simulate both sets of experimental MAS spectra and extract accurate δ_{iso} , C_Q , and η_Q values for each oxygen site. These parameters were then fixed in the

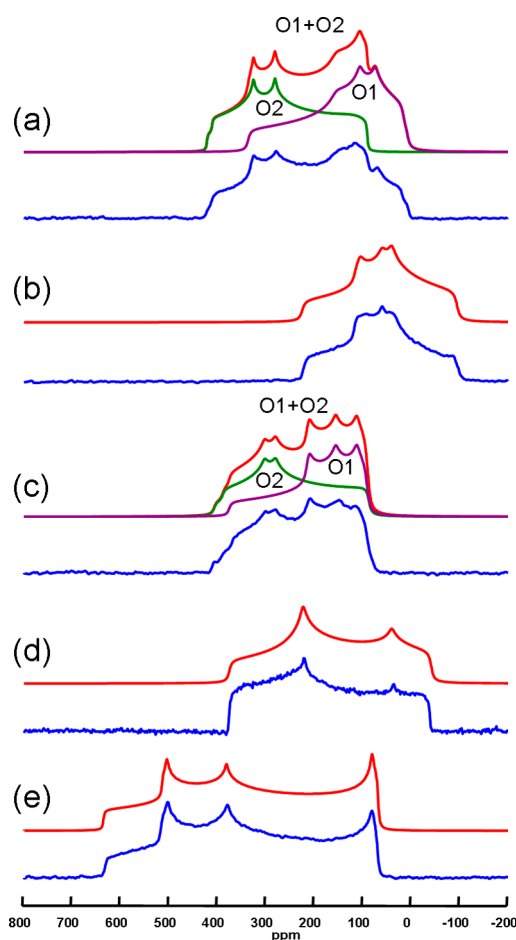


Figure 3. Experimental (lower trace) and simulated (upper trace) ^{17}O NMR spectra at 21.1 T for static samples of (a) $[1,2-^{17}\text{O}_2]\text{SA}$, (b) $[3-^{17}\text{O}]\text{SA}$, (c) $[1,2-^{17}\text{O}_2]\text{Aspirin}$, (d) $[3-^{17}\text{O}]\text{Aspirin}$, and (e) $[4-^{17}\text{O}]\text{Aspirin}$. All spectra were recorded at room temperature. Other experimental parameters are given below. In part a, RD = 10 s, NS = 1792. In part b, RD = 10 s, NS = 4096. In part c, RD = 20 s, NS = 4096. In part d, RD = 2 s, NS = 4096. In part e, RD = 2 s, NS = 4096.

simulations of static spectra, which allowed not only the tensor components to be measured but also the relative orientation between the CS and QC tensors. The general procedure of this kind of spectral analysis was outlined in our previous publications.^{50,51} The experimental static ^{17}O NMR spectra obtained at 21.1 T for SA and Aspirin are shown in Figure 3. Static ^{17}O NMR spectra were also recorded at 14.0 T for the same set of SA and Aspirin samples (given in the Supporting

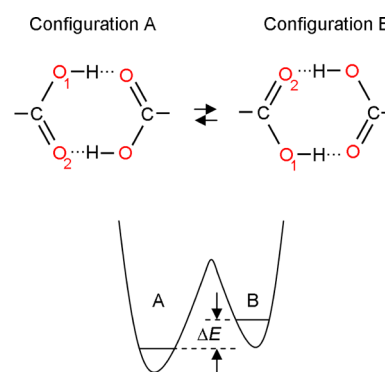


Figure 4. Schematic diagram illustrating the concerted double proton transfer in a carboxylic acid dimer and the corresponding double-well potential curve. The numbering of oxygen atoms is based on the functional group: O_1 for $\text{C}-\text{O}-\text{H}$ and O_2 for $\text{C}=\text{O}$.

Information). Experimental ^{17}O NMR tensor parameters were obtained by simultaneously analyzing the data collected at both magnetic fields; see Table 1. The convention used for the Euler angles (α , β , γ) that describe the relative orientation between the ^{17}O CS and QC tensors can be found in our previous publication.⁵⁰

Now some discussions of the observed ^{17}O NMR tensor parameters in SA and Aspirin are warranted. Most strikingly, the carboxylic acid functional groups in SA and Aspirin exhibit significantly different ^{17}O CS and QC tensor parameters, despite the fact that both form seemingly similar cyclic dimers in the solid state; see Figure 1. For example, the O_1 and O_2 signals in $[1,2-^{17}\text{O}_2]\text{SA}$ have ^{17}O isotropic chemical shifts of 168 and 284 ppm, while the corresponding O_1 and O_2 in $[1,2-^{17}\text{O}_2]\text{Aspirin}$ appear at 215 and 273 ppm. The ^{17}O quadrupole parameters for O_1 and O_2 are also quite different in SA and Aspirin. These large differences will be further examined in detail in the next section. For the phenolic oxygen, O_3 , in SA, the observed ^{17}O QC and CS tensor parameters are similar to those reported for the phenolic oxygens in L-tyrosine^{26,52} and L-tyrosine-HCl^{52–54} but quite different from those found in phenols where hydrogen bonding interactions are absent such as 2-nitro-phenol and 4-nitro-phenol.²⁶ For the O_3 and O_4 atoms in Aspirin, the observed ^{17}O quadrupole parameters are consistent with those reported by Hagaman et al.²⁷ for an ester, methyl-*p*-anisate. However, we also note that the ^{17}O chemical shifts of O_3 and O_4 of Aspirin are considerably higher (more deshielded) than those in methyl-*p*-anisate. This discrepancy can be attributed to the structural difference between the two compounds. In particular,

Table 1. Experimental ^{17}O CS and QC Tensor Parameters for Aspirin and SA^a

compound		δ_{iso} (ppm)	δ_{11} (ppm)	δ_{22} (ppm)	δ_{33} (ppm)	C_Q^b (MHz)	η_Q	α (deg)	β (deg)	γ (deg)
Aspirin	O_1	215	360	208	77	−6.60	0.35	0	90	50
	O_2	273	400	376	43	6.50	0.65	10	90	78
	O_3	203	335	183	91	−9.50	0.60	0	34	0
	O_4	369	608	464	35	8.70	0.20	90	90	58
SA	O_1	168	308	123	73	−7.40	0.16	0	85	144
	O_2	284	425	375	52	7.10	0.45	90	85	72
	O_3	89	162	96	9	−8.30	0.60	90	90	66

^aUncertainties in the experimental tensor parameters were estimated by comparing the quality of fit between observed and simulated spectra: $\delta_{\text{iso}} \pm 1$ ppm, δ_{ii} ($i = 1, 2, 3$) ± 10 ppm, $C_Q \pm 0.05$ MHz, $\eta_Q \pm 0.05$, Euler angles $\pm 10^\circ$. ^bSigns in the experimental C_Q values were assumed to be the same as those from the computations.

Table 2. Computed (CASTEP) ^{17}O CS and QC Tensor Parameters for Aspirin and SA

compound		δ_{iso} (ppm)	δ_{11} (ppm)	δ_{22} (ppm)	δ_{33} (ppm)	C_Q (MHz)	η_Q	
Aspirin (form-I)	configuration A	O1	193.3	355.1	162.7	62.0	−7.402	0.082
		O2	294.2	451.0	419.0	12.4	7.682	0.448
		O3	223.9	381.0	190.0	100.7	−9.832	0.589
		O4	371.2	628.9	469.8	14.9	9.162	0.073
	configuration B	O1	191.3	347.0	158.6	68.3	−7.489	0.101
		O2	313.9	480.8	442.4	18.4	7.802	0.397
		O3	227.9	386.3	197.0	100.4	−9.805	0.598
		O4	377.6	634.0	477.2	21.6	9.167	0.065
Aspirin (form-II) ^a	O1	193.6	355.4	165.3	60.0	−7.388	0.063	
	O2	292.7	450.3	416.7	11.0	7.660	0.454	
	O3	222.6	378.8	188.4	100.8	−9.884	0.586	
	O4	370.1	628.1	468.5	13.6	9.135	0.074	
SA	configuration A	O1	172.8	315.7	146.0	56.8	−7.576	0.172
		O2	262.0	404.1	355.6	26.5	6.628	0.778
		O3	101.4	196.3	122.9	−15.1	−8.286	0.562
	configuration B	O1	188.0	330.8	156.6	76.6	−7.224	0.228
		O2	279.1	427.2	386.4	23.7	7.074	0.616
		O3	107.5	191.0	122.8	8.7	−8.582	0.608

^aOnly results for Aspirin (form-II) in configuration A are shown.

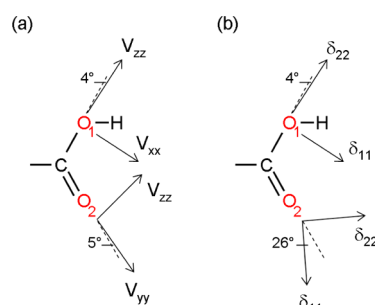


Figure 5. Computed ^{17}O QC (a) and CS (b) tensor orientations in SA and Aspirin. V_{yy} for O_1 and V_{xx} for O_2 are perpendicular to the $\text{O}_1\text{—C—O}_2$ plane. For both O_1 and O_2 , δ_{33} is perpendicular to the $\text{O}_1\text{—C—O}_2$ plane. The numbering of oxygen atoms is based on the functional group: O_1 for C—O—H and O_2 for C=O .

the ester $\text{O}_3\text{—C}_8(\text{=O}_4)$ sp^2 plane in Aspirin is nearly perpendicular to the phenyl plane,^{17–20} whereas the ester plane in methyl-*p*-anisate is very likely to be coplanar with the phenyl plane with the C=O bond being part of a conjugated system.⁵⁵ It has long been known that the ^{17}O chemical shifts of both oxygens in aromatic esters increase with the torsion angle between the ester sp^2 plane and the aromatic ring.⁵⁶ Of course, this apparent correlation is not due to the torsion angle *per se*. Rather, as we have previously explained the parallel trend in ^{13}C NMR,⁵⁷ the origin of this correlation is due to the fact that the π^* molecular orbital that is linked to the paramagnetic shielding contribution through $n \rightarrow \pi^*$ magnetic mixing becomes more localized on the ester functional group when the torsion angle is increased. The carbonyl type oxygen, O_4 , of Aspirin exhibits a very large chemical shift anisotropy, $\delta_{11} - \delta_{33} = 573$ ppm. Compared with other carbonyl compounds, the ^{17}O chemical shift anisotropy found for the carbonyl oxygen in the ester group follows the known trend: aldehyde/ketone > ester \approx amide > carboxylic acid.⁴ While the ether type oxygen, O_3 , has a relatively large $|C_Q|$ value (9.50 MHz), it exhibits a relatively small chemical shift anisotropy ($\delta_{11} - \delta_{33} = 244$ ppm). These

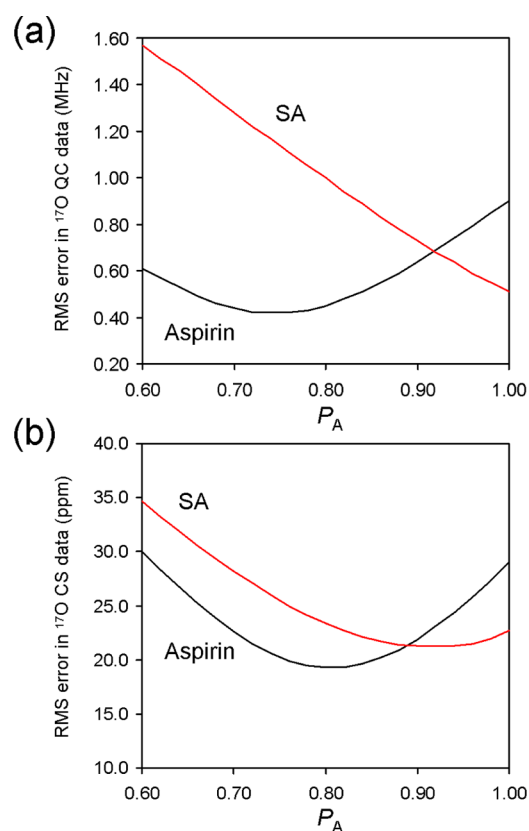


Figure 6. Quality of the data fitting as a function of P_A for (a) ^{17}O QC tensor components (e^2Qq_{ii}/h , $i = x, y, z$) and (b) ^{17}O CS tensor components obtained at 298 K.

appear to be the first set of ^{17}O CS tensors reported for an ester functional group.

3.2. ^{17}O NMR Data Analysis for Carboxylic Acid Dimers. As mentioned earlier, SA and Aspirin form cyclic hydrogen bonded dimers in the crystal lattice; see Figure 4. The concerted double proton transfer in this type of carboxylic acid

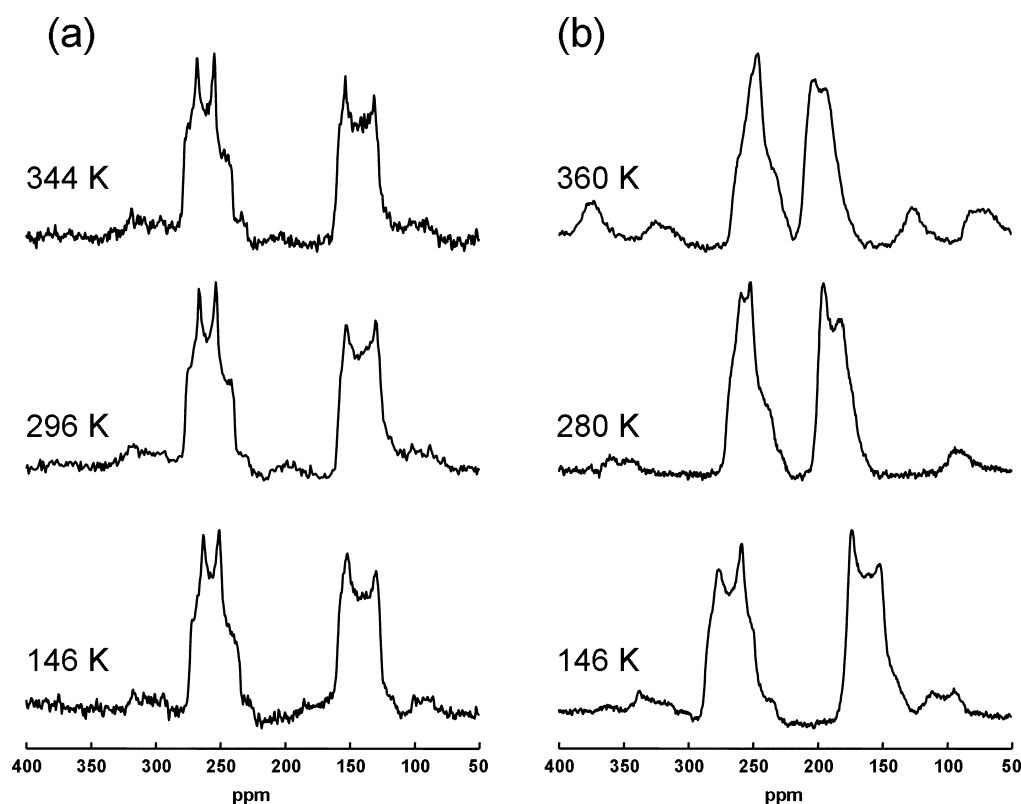


Figure 7. Representative variable-temperature ^{17}O MAS NMR spectra of (a) $[1,2-^{17}\text{O}_2]\text{SA}$ and (b) $[1,2-^{17}\text{O}_2]\text{Aspirin}$ obtained at 21.1 T. The sample spinning frequency was 20 kHz in all cases, except for that of $[1,2-^{17}\text{O}_2]\text{Aspirin}$ at 360 K in which a spinning frequency of 15 kHz was used.

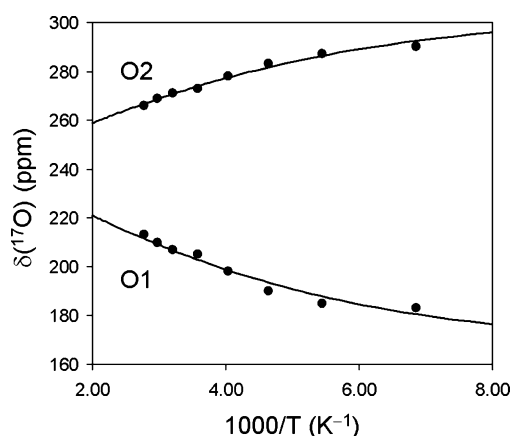


Figure 8. Observed (data points) and best-fit (solid lines) temperature dependent isotropic ^{17}O chemical shifts for O_1 and O_2 in $[1,2-^{17}\text{O}_2]\text{Aspirin}$.

dimers has been well documented in the literature.^{58–68} In general, the double proton transfer occurs on a time scale that is much faster than the NMR Larmor frequency (e.g., 10^8 Hz for ^{17}O at 21.1 T) even at very low temperatures.²⁵ Therefore, all experimental NMR tensors in a carboxylic acid dimer are averaged between the corresponding “rigid” tensors found in configurations A and B, as defined in Figure 4. In general, the two configurations have different energies due to either crystal packing or some intramolecular interactions. As a result, the averaging effect on the two oxygen atoms would lead to two different ^{17}O NMR signals. Following the same procedure as demonstrated by previous workers in analyzing ^1H and ^{13}C NMR data,^{58,59} we can write each observed ^{17}O NMR tensor as

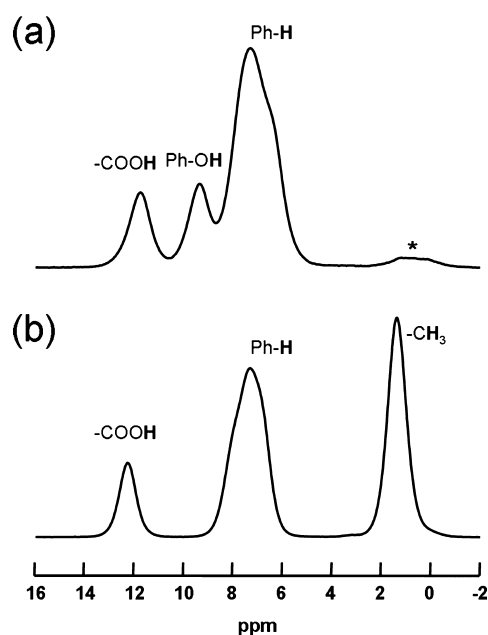


Figure 9. 62.5 kHz ^1H MAS spectra of (a) SA and (b) Aspirin at 21.1 T. A small residual ^1H NMR signal from the probe background is marked by an asterisk.

a weighted average between the two “rigid” tensors found in configurations A and B. If we use the shielding tensor (σ) as an example, we have

$$\sigma_1^{\text{obs}} = P_A \sigma_{\text{C=O}}^{\text{A}} + P_B \sigma_{\text{C-OH}}^{\text{B}} \quad (1)$$

$$\sigma_2^{\text{obs}} = P_A \sigma_{\text{C-OH}}^{\text{A}} + P_B \sigma_{\text{C=O}}^{\text{B}} \quad (2)$$

Table 3. Experimental and Computed (CASTEP) ^{13}C and ^1H Isotropic Chemical Shifts (in ppm) for Aspirin and SA in the Solid State^a

compound	atom	experiment	CASTEP	
			form-I	form-II
Aspirin	C1	122.11	128.13	128.28
	C2	152.87	163.79	163.54
	C3	125.51	132.13	132.77
	C4	138.32	146.89	146.44
	C5	127.64	135.27	135.22
	C6	134.80	142.65	142.07
	C7	170.70	180.23	180.21
	C8	171.85	184.43	183.65
	C9	19.75	21.79	23.57
	COOH	12.3	14.5	14.9
	Ph-H	7.2	7.8	7.7
	CH ₃	1.4	1.6	1.1
SA	C1	112.02	117.16	
	C2	162.18	171.58	
	C3	118.46	124.43	
	C4	138.70	146.40	
	C5	121.02	126.83	
	C6	133.20	139.90	
	C7	176.05	184.31	
	COOH	11.7	13.8	
	Ph-H	9.3	11.1	
	Ph-OH	7.2	7.4	

^aOnly computational results for SA and Aspirin in configuration A are shown.

where P_A and P_B are the probabilities of finding the system in configurations A and B, respectively. If the energy asymmetry of the double-well potential curve between configurations A and B is defined as ΔE , we have

$$P_A = \frac{e^{\Delta E/RT}}{1 + e^{\Delta E/RT}}; \quad P_B = 1 - P_A \quad (3)$$

where R is the gas constant and T is the absolute temperature of the system. It is important to recognize that the averaging in the above equations occurs between *tensor* quantities. This can be readily done by taking a weighted average of individual tensor matrix elements in a common frame of reference followed by diagonalization of the averaged tensor to yield the principal components. Since ^{17}O NMR tensors may be different in the two configurations, it is necessary to compute them for both configurations. For configuration B, we first manually moved the two protons and then performed full geometry optimization using CASTEP. Although all atoms were relaxed during the geometry optimization, the two protons did not return to their original positions found in configuration A, suggesting that configuration B is a true local minimum. After establishing the proper crystal structures for configurations A and B, we calculate the ^{17}O QC and CS tensors for both configurations A and B for SA and Aspirin; see Table 2. For comparison, we also listed in Table 2 the computational results for Aspirin (form-II). The computed ^{17}O NMR tensor orientations for O_1 and O_2 in SA and Aspirin are illustrated in Figure 5. It is clear that both ^{17}O QC and CS tensors change their orientations as a result of the double proton transfer. Therefore, it is important to treat the whole tensor in the averaging process. Now we can determine the value of P_A by

using eqs 1 and 2. As seen from Figure 6, the best-fit P_A values for Aspirin are 0.74 ± 0.02 and 0.82 ± 0.02 from analyses of ^{17}O QC and CS tensor components, respectively. Thus, we report a mean value of P_A for Aspirin, 0.78 ± 0.04 . For SA, it is more difficult to estimate the best-fit P_A , as it is very close to 1. Nonetheless, combining the ^{17}O QC and CS data shown in Figure 6, we estimate a mean value of P_A for SA, 0.98 ± 0.02 . These results suggest that the SA dimer exhibits a much larger energy asymmetry than does the Aspirin dimer. Our P_A value for Aspirin is in excellent agreement with that found from an analysis of ^{17}O NQR data, $P_A = 0.77$ at 291 K.³³ For SA, there does not appear to be any report on P_A in the literature.

To further confirm the above data analyses and, more importantly, to obtain accurate values of ΔE , we recorded VT ^{17}O MAS spectra for both $[1,2-^{17}\text{O}_2]\text{SA}$ and $[1,2-^{17}\text{O}_2]\text{Aspirin}$ at 21.1 T. As seen from Figure 7, while the ^{17}O MAS spectra of $[1,2-^{17}\text{O}_2]\text{SA}$ exhibit very little temperature dependence, those for $[1,2-^{17}\text{O}_2]\text{Aspirin}$ are highly temperature dependent. In particular, as the temperature is increased, the two peaks observed for Aspirin move gradually toward each other. In addition, the ^{17}O QC parameters (line shapes) change considerably as a function of temperature. For example, the values of η_Q for the two peaks are 0.35 and 0.05 at 146 K, and they change to 0.80 and 0.25 at 360 K. For both sites, the values of C_Q also decrease by approximately 20% as the temperature is increased from 146 to 360 K. Using the averaging procedure described in eqs 1–3, together with the CASTEP data shown in Table 2, we were able to fit the observed temperature dependent isotropic ^{17}O chemical shifts, as shown in Figure 8, and extract an accurate value of ΔE for Aspirin, 3.0 ± 0.5 kJ/mol. The isotropic ^{17}O chemical shifts for the two sites change more than 25 ppm between 146 and 360 K.

For SA, as no obvious temperature dependence was observed, only a lower limit for ΔE can be estimated, $\Delta E > 10$ kJ/mol, on the basis of the aforementioned best-fit P_A value of 0.98 at 298 K. These experimental data on the energy asymmetry are in good agreement with the results from our plane-wave DFT computations: $\Delta E = 17.8$ kJ/mol for SA and $\Delta E = 3.7$ kJ/mol for Aspirin. Previously, ΔE values for carboxylic acid dimers were found to lie in a range from ~ 0.5 kJ/mol in benzoic acid⁵⁸ to 3.4 kJ/mol in malonic acid⁶⁹ to 5.9 kJ/mol in β -oxalic acid.³³ Thus, while the energy asymmetry found in Aspirin appears to be in the middle of the range, the energy asymmetry in SA is so large that the proton dynamics is significantly hindered. It is particularly interesting to further compare SA with other related derivatives of benzoic acid. For 4-substituted benzoic acids, the ΔE values are all approximately 1 kJ/mol.^{70,71} For 2-nitrobenzoic acid, the value of ΔE increases to 5.8 kJ/mol.⁷² It is clear that the very large ΔE value in SA is due to the formation of an intramolecular $\text{O}_3\cdots\text{H}\cdots\text{O}_2$ hydrogen bond that strongly favors configuration A, in which $\text{C}=\text{O}_2$ and $\text{O}_3\cdots\text{H}$ are on the same side of the molecule; see Figure 1. Our observations of very different ΔE values in SA and Aspirin are also consistent with the neutron diffraction data. More specifically, Bacon and Jude¹⁶ reported that the acid proton in SA exhibits a normal thermal B factor (3.78 \AA^2). In contrast, Wilson^{19,20} observed significant elongation of the thermal ellipsoid for the acid proton in Aspirin above 200 K, which can be modeled by proton dynamics within an asymmetric double-well potential.

3.3. Comparison between Experimental and Computed NMR Parameters. After establishing a proper averaging model for data analysis in the previous section, we

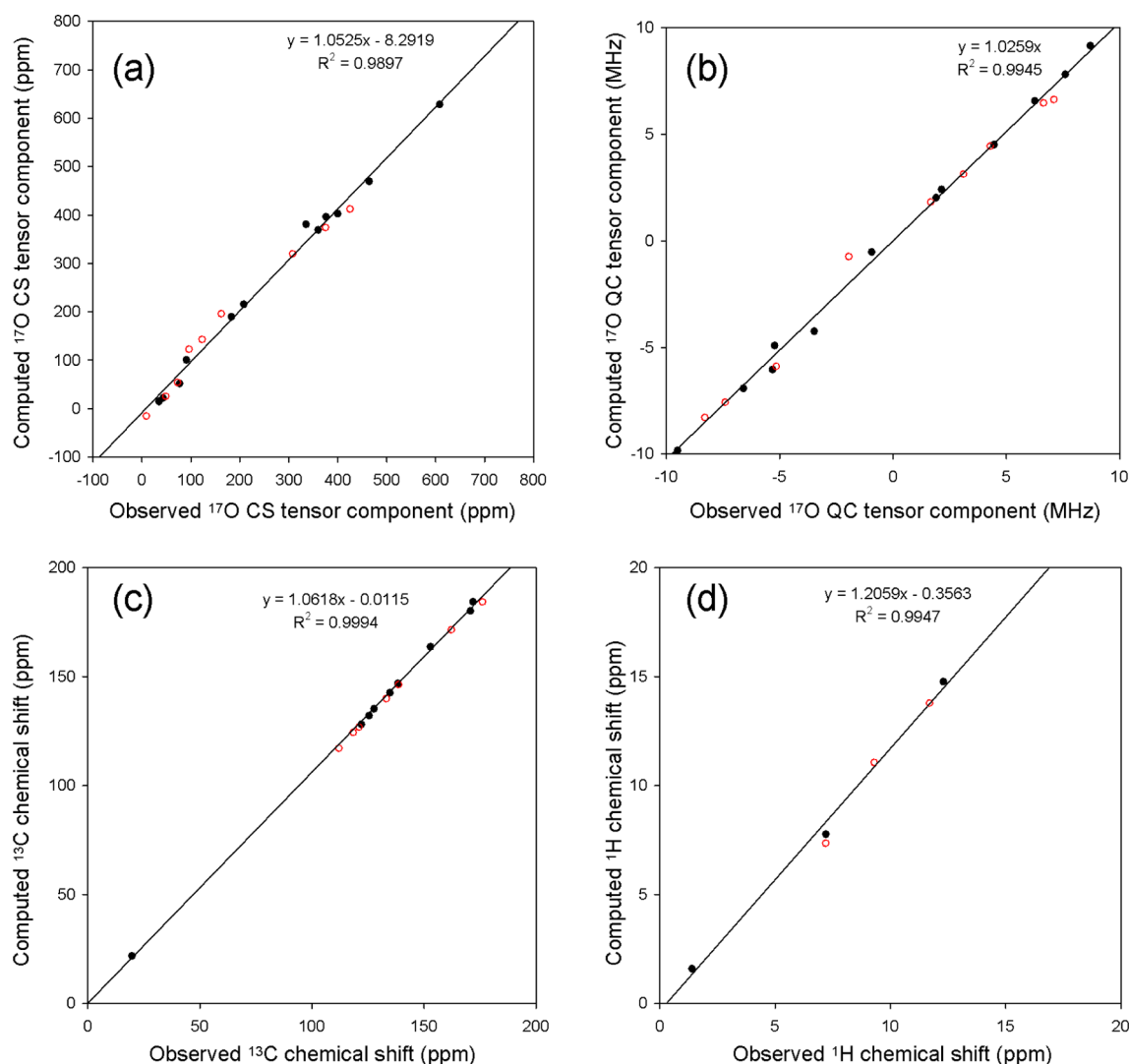


Figure 10. Correlations between experimental and CASTEP-computed (a) ^{17}O CS tensor components, (b) ^{17}O QC tensor components (e^2Qq_{ii}/h , $i = x, y, z$), (c) isotropic ^{13}C chemical shifts, and (d) isotropic ^1H chemical shifts for SA (open circles) and Aspirin (close circles).

now can quantitatively compare the experimental and computed ^{17}O NMR tensors for all oxygen sites found in SA and Aspirin. For completeness, we also recorded ^{13}C CP/MAS NMR spectra (given in the Supporting Information) and ^1H very fast MAS NMR spectra (shown in Figure 9) for SA and Aspirin. It is important to point out that the ^{13}C CP/MAS NMR spectra were also used to confirm the structural polymorph of each solid sample. This step ensures that a comparison between experimental and computed NMR parameters is meaningful. The experimental solid-state ^{13}C and ^1H chemical shifts for SA and Aspirin are given in Table 3. Here it is worth noting that all NMR parameters computed for the two Aspirin polymorphs (form-I and form-II) are very similar. This finding is not unexpected, as the crystal structures of the two polymorphs exhibit only very subtle differences, as explained previously.^{21–23} Interestingly, our plane-wave DFT computations suggest that the largest detectable difference between form-I and form-II occurs on the ^{13}C chemical shift for the methyl group, C9, with a chemical shift difference of 1.78 ppm between the two polymorphs. This result is consistent with a previous report where the ^{13}C CP/MAS spectrum of a lyophilized Aspirin sample shows splitting in the methyl signal.⁷³ Perhaps this spectral feature could be used as an

“NMR spectral signature” for differentiating between the two Aspirin polymorphs.

Now that we have obtained solid-state NMR parameters for all magnetic nuclei in SA and Aspirin, we can evaluate the accuracy of the computational results for these nuclei simultaneously. As seen from Figure 10, the overall agreement between experimental and computed results is excellent. It should be noted that, in Figure 10a and b, the computed ^{17}O NMR tensor components for O_1 and O_2 of Aspirin are the “averaged” values as outlined in the previous section rather than the “rigid” values shown in Table 2. For the ^{17}O QC and CS tensor components, the root-mean-squared (RMS) errors are approximately 0.4 MHz and 20 ppm, respectively. We should note that the experimental uncertainties in experimental tensor components are considerably larger than those for the isotropic values. For the isotropic ^{13}C and ^1H chemical shifts, the RMS errors are 7.9 and 1.5 ppm, respectively. However, these RMS errors are reduced to 2.4 and 0.9 ppm after the nonunitary slopes are corrected.⁷⁴ Recently, Esrafil and co-workers^{75–77} computed NMR parameters in SA and Aspirin using a molecular cluster approach. A comparison of our results and theirs clearly suggests that the plane-wave DFT is a far better method than the cluster approach for predicting solid-state

NMR parameters. The ultimate accuracy of the plane-wave DFT computational results may also be sensitive to fast molecular motions, as recently demonstrated by Dracinsky and Hodgkinson.⁷⁸ Finally, we briefly discuss some experimental ²H quadrupole coupling data reported for SA and Aspirin. Clymer and Ragle³² reported C_Q and η_Q values of 216.8 kHz and 0.141 for the phenolic deuteron and 174.2 kHz and 0.158 for the carboxylic deuteron in SA at 77 K. Our plane-wave DFT calculations yielded the following results for SA: phenolic deuteron, $C_Q = 203.7$ kHz and $\eta_Q = 0.154$; carboxylic deuteron, $C_Q = 153.0$ kHz and $\eta_Q = 0.166$. For Aspirin, Poplett and Smith³¹ reported that $C_Q = 173.1$ kHz and $\eta_Q = 0.143$ for the carboxylic deuteron at 291 K, which can be compared with our plane-wave DFT results: $C_Q = 141.6$ kHz and $\eta_Q = 0.167$. In general, we found a reasonable agreement between experimental and computed ²H quadrupole parameters for SA and Aspirin.

4. SUMMARY

We have reported synthesis and solid-state ¹⁷O NMR results for five site-specifically ¹⁷O-labeled samples of SA and Aspirin. Carefully designed synthetic procedures ensured highly selective ¹⁷O-labeling at the desired oxygen sites in SA and Aspirin, and excellent yields were achieved in most cases. High-quality solid-state ¹⁷O NMR spectra obtained at two magnetic fields allowed us to extract a complete set of reliable ¹⁷O QC and CS tensor parameters in these important pharmaceutical compounds. We demonstrated that it is important to take into consideration the averaging effect due to concerted double proton transfer in carboxylic acid dimers in order to compare experimental and computed ¹⁷O NMR tensors for carboxylic acid functional groups. Further, we showed that a careful analysis of variable temperature ¹⁷O NMR spectra of Aspirin provided an accurate measure of the energy asymmetry between the two energy minima in the double-well potential. Using experimental NMR parameters observed for all magnetic nuclei (¹⁷O, ¹³C, and ¹H) in SA and Aspirin, we found that the plane-wave DFT computations are highly accurate for predicting NMR parameters for these light elements in well-defined crystalline organic solids. It is possible to extend the present study to other pharmaceutical materials including cocrystals. Now that we have successfully made site-specifically ¹⁷O-labeled SA and Aspirin, it is also possible to use ¹⁷O NMR to probe the binding of these molecules to biological macromolecules. Research in this direction is underway in our laboratory.

■ ASSOCIATED CONTENT

Supporting Information

Experimental and simulated static ¹⁷O NMR spectra of five samples of SA and Aspirin obtained at 14.0 T. Experimental ¹³C CP/MAS spectra for seven different samples of SA and Aspirin. A complete set of VT ¹⁷O MAS spectra for [1,2-¹⁷O₂]Aspirin at 21.1 T. Two tables listing bond lengths in various X-ray, neutron diffraction, and CASTEP-optimized crystal structures of SA and Aspirin. This material is available free of charge via the Internet at <http://pubs.acs.org>.

■ AUTHOR INFORMATION

Corresponding Author

*E-mail: gang.wu@chem.queensu.ca.

Notes

The authors declare no competing financial interest.

■ ACKNOWLEDGMENTS

This work was supported by the Natural Sciences and Engineering Research Council (NSERC) of Canada. Access to the 900 MHz NMR spectrometer and CASTEP software was provided by the National Ultrahigh-Field NMR Facility for Solids (Ottawa, Canada), a national research facility funded by the Canada Foundation for Innovation, the Ontario Innovation Trust, Recherche Québec, the National Research Council Canada, and Bruker BioSpin and managed by the University of Ottawa (<http://nmr900.ca>). NSERC is also acknowledged for a Major Resources Support grant. Variable-temperature ¹⁷O MAS NMR spectra at 21.1 T were acquired at the National High Magnetic Field Laboratory, which is supported by the National Science Foundation, the State of Florida, and the US Department of Energy. We also thank anonymous reviewers for helpful suggestions.

■ REFERENCES

- (1) Ashbrook, S. E.; Smith, M. E. Solid State ¹⁷O NMR – An Introduction to the Background Principles and Applications to Inorganic Materials. *Chem. Soc. Rev.* **2006**, 35, 718–735.
- (2) Ashbrook, S. E.; Smith, M. E. In *NMR of Quadrupolar Nuclei in Solid Materials*; Wasylishen, R. E., Ashbrook, S. E., Wimperis, S., Eds.; John Wiley & Sons, Ltd.: Chichester, U.K., 2012; pp 291–320.
- (3) Lemaître, V.; Smith, M. E.; Watts, A. A Review of Oxygen-17 Solid-State NMR of Organic Materials - Towards Biological Applications. *Solid State Nucl. Magn. Reson.* **2004**, 26, 215–235.
- (4) Wu, G. Solid-State ¹⁷O NMR Studies of Organic and Biological Molecules. *Prog. Nucl. Magn. Reson. Spectrosc.* **2008**, 52, 118–169.
- (5) Wu, G. In *NMR of Quadrupolar Nuclei in Solid Materials*; Wasylishen, R. E., Ashbrook, S. E., Wimperis, S., Eds.; John Wiley & Sons, Ltd.: Chichester, U.K., 2012; pp 273–290.
- (6) Zhu, J.; Kwan, I. C. M.; Wu, G. Quadrupole-Central-Transition ¹⁷O NMR Spectroscopy of Protein-Ligand Complexes in Solution. *J. Am. Chem. Soc.* **2009**, 131, 14206–14207.
- (7) Zhu, J.; Ye, E.; Tersikh, V.; Wu, G. Solid-State ¹⁷O NMR Spectroscopy of Large Protein-Ligand Complexes. *Angew. Chem., Int. Ed.* **2010**, 49, 8399–8402.
- (8) Zhu, J.; Wu, G. Quadrupole Central Transition ¹⁷O NMR Spectroscopy of Biological Macromolecules in Aqueous Solution. *J. Am. Chem. Soc.* **2011**, 133, 920–932.
- (9) Kong, X.; O'Dell, L. A.; Tersikh, V.; Ye, E.; Wang, R.; Wu, G. Variable-Temperature ¹⁷O NMR Studies Allow Quantitative Evaluation of Molecular Dynamics in Organic Solids. *J. Am. Chem. Soc.* **2012**, 134, 14609–14617.
- (10) Michaelis, V. K.; Markhasin, E.; Daviso, E.; Herzfeld, J.; Griffin, R. G. Dynamic Nuclear Polarization of Oxygen-17. *J. Phys. Chem. Lett.* **2012**, 3, 2030–2034.
- (11) Blanc, F.; Sperrin, L.; Jefferson, D. A.; Pawsey, S.; Rosay, M.; Grey, C. P. Dynamic Nuclear Polarization Enhanced Natural Abundance ¹⁷O Spectroscopy. *J. Am. Chem. Soc.* **2013**, 135, 2975–2978.
- (12) Jeffreys, D. *Aspirin: The Remarkable Story of a Wonder Drug*; Bloomsbury Publishing: New York, 2005.
- (13) Data from Web of Science.
- (14) Cochran, W. The Crystal and Molecular Structure of Salicylic Acid. *Acta Crystallogr.* **1953**, 6, 260–268.
- (15) Sundaralingam, M.; Jesen, L. H. Refinement of the Structure of Salicylic Acid. *Acta Crystallogr.* **1965**, 18, 1053–1058.
- (16) Bacon, G. E.; Jude, R. J. Neutron-Diffraction Studies of Salicylic Acid and α -Resorcinol. *Z. Kristallogr.* **1973**, 138, 19–40.
- (17) Wheatley, P. J. The Crystal and Molecular Structure of Aspirin. *J. Chem. Soc.* **1964**, 6036–6048.

- (18) Kim, Y.; Machida, K.; Taga, T.; Osaki, K. Structure Redetermination and Packing Analysis of Aspirin Crystal. *Chem. Pharm. Bull.* **1985**, *33*, 2641–2647.
- (19) Wilson, C. C. Hydrogen Atoms in Acetylsalicylic Acid (Aspirin): The Librating Methyl Group and Probing the Potential Well in the Hydrogen-Bonded Dimer. *Chem. Phys. Lett.* **2001**, *335*, 57–63.
- (20) Wilson, C. C. Interesting Proton Behaviour in Molecular Structures. Variable Temperature Neutron Diffraction and Ab Initio Study of Acetylsalicylic Acid: Characterising Librational Motions and Comparing Protons in Different Hydrogen Bonding Potentials. *New J. Chem.* **2002**, *26*, 1733–1739.
- (21) Vishweshwar, P.; McMahon, J. A.; Oliveira, M.; Peterson, M. L.; Zaworotko, M. The Predictably Elusive Form II of Aspirin. *J. Am. Chem. Soc.* **2005**, *127*, 16802–16803.
- (22) Bond, A. D.; Boese, R.; Desiraju, G. R. On the Polymorphism of Aspirin. *Angew. Chem., Int. Ed.* **2007**, *46*, 615–617.
- (23) Bond, A. D.; Boese, R.; Desiraju, G. R. On the Polymorphism of Aspirin: Crystalline Aspirin as Intergrowths of Two “Polymorphic” Domains. *Angew. Chem., Int. Ed.* **2007**, *46*, 618–622.
- (24) Bond, A. D.; Solanko, K. A.; Parsons, S.; Redder, S.; Boese, R. Single Crystals of Aspirin Form II: Crystallisation and Stability. *CrystEngComm* **2011**, *13*, 399–401.
- (25) Horsewill, A. J. Quantum Tunnelling in the Hydrogen Bond. *Prog. Nucl. Magn. Reson. Spectrosc.* **2008**, *52*, 170–196.
- (26) Dong, S.; Yamada, K.; Wu, G. Oxygen-17 Nuclear Magnetic Resonance of Organic Solids. *Z. Naturforsch., A* **2000**, *55*, 21–28.
- (27) Hagaman, E.; Chen, B.; Jiao, J.; Parsons, W. Solid-State ^{17}O NMR Study of Benzoic Acid Adsorption on Metal Oxide Surfaces. *Solid State Nucl. Magn. Reson.* **2012**, *41*, 60–67.
- (28) Chang, C.; Diaz, L. E.; Morin, F.; Grant, D. M. Solid-State ^{13}C NMR Study of Drugs: Aspirin. *Magn. Reson. Chem.* **1986**, *24*, 768–771.
- (29) Diaz, L. E.; Frydman, L.; Olivieri, A. C.; Frydman, B. Solid State NMR of Drugs: Soluble Aspirin. *Anal. Lett.* **1987**, *20*, 1657–1666.
- (30) Kitchin, S. J.; Halstead, T. K. Solid-State ^2H NMR Studies of Methyl Group Dynamics in Aspirin and Aspirin · β -Cyclodextrin. *Appl. Magn. Reson.* **1999**, *17*, 283–300.
- (31) Poplett, I. J. F.; Smith, J. A. S. ^{17}O and ^2H Quadrupole Double Resonance in Some Carboxylic Acid Dimers. *J. Chem. Soc., Faraday Trans. 2* **1981**, *77*, 1473–1485.
- (32) Clymer, J. W.; Ragle, J. L. Deuterium Quadrupole Coupling in Methanol, Salicylic Acid, Catechol, Resorcinol, and Hydroquinone. *J. Chem. Phys.* **1982**, *77*, 4366–4373.
- (33) Gough, A.; Haq, M. M. I.; Smith, J. A. S. The Mechanism of Proton Transfer in Carboxylic Acid Dimers as Studied by ^{17}O Quadrupole Double Resonance. *Chem. Phys. Lett.* **1985**, *117*, 389–393.
- (34) Harris, R. K. Applications of Solid-State NMR to Pharmaceutical Polymorphism and Related Matters. *J. Pharm. Pharmacol.* **2007**, *59*, 225–239.
- (35) Geppi, M.; Mollica, G.; Borsacchi, S.; Veracini, C. A. Solid-State NMR Studies of Pharmaceutical Systems. *Appl. Spectrosc. Rev.* **2008**, *4*, 202–302.
- (36) Salager, E.; Day, G. M.; Stein, R. S.; Pickard, C. J.; Elena, B.; Emsley, L. Powder Crystallography by Combined Crystal Structure Prediction and High-Resolution ^1H Solid-State NMR. *J. Am. Chem. Soc.* **2010**, *132*, 2564–2566.
- (37) Brown, S. P. Applications of High-Resolution ^1H Solid-State NMR. *Solid State Nucl. Magn. Reson.* **2012**, *41*, 1–27.
- (38) Baías, M.; Widdifield, C. M.; Dumez, J. -N.; Thompson, H. P. G.; Cooper, T. G.; Salager, E.; Bassil, S.; Stein, R. S.; Lesage, A.; Day, G. M.; Emsley, L. Powder Crystallography of Pharmaceutical Materials by Combined Crystal Structure Prediction and Solid-State ^1H NMR Spectroscopy. *Phys. Chem. Chem. Phys.* **2013**, *15*, 8069–8080.
- (39) Tatton, A. S.; Pham, T. N.; Vogt, F. G.; Iuga, D.; Edwards, A. J.; Brown, S. P. Probing Intermolecular Interactions and Nitrogen Protonation in Pharmaceuticals by Novel N-15-Edited and 2D N-14-H-1 Solid-State NMR. *CrystEngComm* **2012**, *14*, 2654–2659.
- (40) Tatton, A. S.; Pham, T. N.; Vogt, F. G.; Iuga, D.; Edwards, A. J.; Brown, S. P. Probing Hydrogen Bonding in Cocrystals and Amorphous Dispersions Using ^{14}N – ^1H HMQC Solid-State NMR. *Mol. Pharmacol.* **2013**, *10*, 999–1007.
- (41) Burgess, K. M. N.; Perras, F. A.; Lebrun, A.; Messner-Henning, E.; Korobkov, I.; Bryce, D. L. Sodium-23 Solid-State Nuclear Magnetic Resonance of Commercial Sodium Naproxen and Its Solvates. *J. Pharm. Sci.* **2012**, *101*, 2930–2940.
- (42) Hamaed, H.; Pawlowski, J. M.; Cooper, B. F. T.; Fu, F.; Eichhorn, S. H.; Schurko, R. W. Application of Solid-State ^{35}Cl NMR to the Structural Characterization of Hydrochloride Pharmaceuticals and Their Polymorphs. *J. Am. Chem. Soc.* **2008**, *130*, 11056–11065.
- (43) Perras, F. A.; Bryce, D. L. Direct Investigation of Covalently Bound Chlorine in Organic Compounds by Solid-State ^{35}Cl NMR Spectroscopy and Exact Spectral Line-Shape Simulations. *Angew. Chem., Int. Ed.* **2012**, *51*, 4227–4230.
- (44) Massiot, D.; Fayon, F.; Capron, M.; King, I.; Le Calvé, S.; Alonso, B.; Durand, J. O.; Bujoli, B.; Gan, Z.; Hoatson, G. Modelling One and Two-Dimensional Solid-State NMR Spectra. *Magn. Reson. Chem.* **2002**, *40*, 70–76.
- (45) Clark, S. J.; Segall, M. D.; Pickard, C. J.; Hasnip, P. J.; Probert, M. J.; Refson, K.; Payne, M. C. First Principles Methods Using CASTEP. *Z. Kristallogr.* **2005**, *220*, 567–570.
- (46) Montis, R.; Hursthouse, M. B. Surprisingly Complex Supramolecular Behaviour in the Crystal Structures of a Family of Mono-Substituted Salicylic Acid. *CrystEngComm* **2012**, *14*, 5242–5254.
- (47) Pickard, C. J.; Mauri, F. All-Electron Magnetic Response with Pseudopotentials: NMR Chemical Shifts. *Phys. Rev. B* **2001**, *63*, 245101.
- (48) Yates, J. R.; Pickard, C. J.; Mauri, F. Calculation of NMR Chemical Shifts for Extended Systems Using Ultrasoft Pseudopotentials. *Phys. Rev. B* **2007**, *76*, 024401.
- (49) Wong, A.; Smith, M. E.; Terskikh, V.; Wu, G. Obtaining Accurate Chemical Shifts for All Magnetic Nuclei (^1H , ^{13}C , ^{17}O , and ^{27}Al) in Tris(2, 4-pentanedionato-O, O')aluminium (III)—A Solid-State NMR Case Study. *Can. J. Chem.* **2011**, *89*, 1087–1094.
- (50) Yamada, K.; Dong, S.; Wu, G. Solid-State ^{17}O NMR Investigation of the Carbonyl Oxygen Electric-Field-Gradient Tensor and Chemical Shielding Tensor in Amides. *J. Am. Chem. Soc.* **2000**, *122*, 11602–11609.
- (51) Wu, G.; Dong, S.; Ida, R.; Reen, N. A Solid-State ^{17}O Nuclear Magnetic Resonance Study of Nucleic Acid Bases. *J. Am. Chem. Soc.* **2002**, *124*, 1768–1777.
- (52) Zhu, J.; Lau, J. Y. C.; Wu, G. A Solid-State ^{17}O NMR Study of L-Tyrosine in Different Ionization States: Implications for Probing Tyrosine Side Chains in Proteins. *J. Phys. Chem. B* **2010**, *114*, 11681–11688.
- (53) Pike, K. J.; Lemaitre, V.; Kukol, A.; Anupold, T.; Samoson, A.; Howes, A. P.; Watts, A.; Smith, M. E.; Dupree, R. Solid-State ^{17}O NMR of Amino Acids. *J. Phys. Chem. B* **2004**, *108*, 9256–9263.
- (54) Brinkmann, A.; Kentgens, A. P. M. Sensitivity Enhancement and Heteronuclear Distance Measurements in Biological ^{17}O Solid-State NMR. *J. Phys. Chem. B* **2006**, *110*, 16089–16101.
- (55) While the crystal structure of methyl-*p*-anisate has not been reported in the literature, two closely related anisate derivatives show that, in each case, the ester plane is nearly coplanar with the aromatic ring: (a) Xiao, Z.; Fang, R.; Shi, L.; Ding, H.; Xu, C.; Zhu, H. *Can. J. Chem.* **2007**, *85*, 951. (b) Saeed, A.; Khera, R. A.; Bolte, M. *Acta Crystallogr.* **2007**, *63E*, o4582.
- (56) Boykin, D. W.; Baumstark, A. L. In *^{17}O NMR Spectroscopy in Organic Chemistry*; Boykin, D. W., Ed.; CRC Press: Boca Raton, FL, 1991; Chapter 3.
- (57) Wu, G.; Lumsden, M. D.; Ossenkamp, G. C.; Eichele, K.; Wasylshen, R. E. Carbonyl Carbon Chemical Shift Tensors for a Typical Aryl Aldehyde and Formaldehyde. NMR Studies of the Isolated ^{13}C – ^2H Spin Pair of 3,4-Dibenzoyloxybenzaldehyde- $^{13}\text{C}_\alpha$ – $^2\text{H}_\alpha$. *J. Phys. Chem.* **1995**, *99*, 15806–15813.
- (58) Nagaoka, S.; Terao, T.; Imashiro, F.; Saika, A.; Hirota, N.; Hayashi, S. A Study on the Proton Transfer in the Benzoic Acid Dimer by ^{13}C High-Resolution Solid-State NMR and Proton T_1 Measurement. *Chem. Phys. Lett.* **1981**, *80*, 580–525.

- (59) Meier, B. H.; Graf, F.; Ernst, R. R. Structure and Dynamics of Intramolecular Hydrogen Bonds in Carboxylic Acid Dimers: A Solid State NMR Study. *J. Chem. Phys.* **1982**, *76*, 767–774.
- (60) Nagaoka, S.; Terao, T.; Imashiro, F.; Saika, A.; Hirota, N.; Hayashi, S. An NMR Relaxation Study on the Proton Transfer in the Hydrogen Bonded Carboxylic Acid Dimers. *J. Chem. Phys.* **1983**, *79*, 4694–4703.
- (61) Jarvie, T. P.; Thayer, A. M.; Millar, J. M.; Pines, A. Effect of Correlated Proton Jumps on the Zero-Field NMR-Spectrum of Solid P-Toluic Acid. *J. Chem. Phys.* **1987**, *91*, 2240–2242.
- (62) Oppenländer, A.; Rambaud, C.; Trommsdorff, H. P.; Vial, J.-C. Translational Tunneling of Protons in Benzoic-Acid Crystals. *Phys. Rev. Lett.* **1989**, *63*, 1432–1435.
- (63) Stöckli, A.; Meier, B. H.; Kreis, R.; Meyer, R.; Ernst, R. R. Hydrogen Bond Dynamics in Isotopically Substituted Benzoic Acid Dimers. *J. Chem. Phys.* **1990**, *93*, 1502–1520.
- (64) Wilson, C. C.; Shankland, N.; Florence, A. J. A Single-Crystal Neutron Diffraction Study of the Temperature Dependence of Hydrogen-Atom Disorder in Benzoic Acid Dimers. *J. Chem. Soc., Faraday Trans.* **1996**, *92*, 5051–5057.
- (65) Brougham, D. F.; Horsewill, A. J.; Ikram, A.; Ibberson, R. M.; McDonald, P. J.; Pinter-Krainer, M. The Correlation between Hydrogen Bond Tunneling Dynamics and the Structure of Benzoic Acid Dimers. *J. Chem. Phys.* **1996**, *105*, 979–982.
- (66) Neumann, M.; Brougham, D. F.; McGloin, C. J.; Johnson, M. R.; Horsewill, A. J.; Trommsdorff, H. P. Proton Tunneling in Benzoic Acid Crystals at Intermediate Temperatures: Nuclear Magnetic Resonance and Neutron Scattering Studies. *J. Chem. Phys.* **1998**, *109*, 7300–7311.
- (67) Jenkinson, R. I.; Ikram, A.; Horsewill, A. J.; Trommsdorff, H. P. The Quantum Dynamics of Proton Transfer in Benzoic Acid Measured by Single Crystal NMR Spectroscopy and Relaxometry. *Chem. Phys.* **2003**, *294*, 95–104.
- (68) Xue, Q.; Horsewill, A. J.; Johnson, M. R.; Trommsdorff, H. P. Isotope Effects Associated with Tunneling and Double Proton Transfer in the Hydrogen Bonds of Benzoic Acid. *J. Chem. Phys.* **2004**, *120*, 11107–11119.
- (69) Idziak, S.; Pislewski, N. An NMR Relaxation Study on the Hydrogen Dynamics in Malonic Acid. *Chem. Phys.* **1987**, *111*, 439–443.
- (70) Seliger, J.; Zagar, V. ^{17}O Nuclear Quadrupole Resonance Study of Proton Disorder in Solid Benzoic Acid, 4-Hydroxybenzoic Acid and 4-Nitrobenzoic Acid. *Chem. Phys. Lett.* **1998**, *234*, 223–230.
- (71) Horsewill, A. J.; McGloin, C. J.; Trommsdorff, H. P.; Johnson, M. R. Proton Tunnelling in the Hydrogen Bonds of Halogen-Substituted Derivatives of Benzoic Acid Studied by NMR Relaxometry: The Case of Large Energy Asymmetry. *Chem. Phys.* **2003**, *291*, 41–52.
- (72) Torkar, M.; Zagar, V.; Seliger, J. ^1H - ^{17}O Nuclear-Quadrupole Double-Resonance Study of Hydrogen Disorder in 2-Nitrobenzoic Acid. *J. Magn. Reson.* **2000**, *144*, 13–19.
- (73) Sperger, D.; Chen, B.; Offerdahl, T.; Hong, S.; Schieber, L.; Lubach, J.; Munson, E. Effects of Processing on Bulk Aspirin and Aspirin Formulations. *AAPS J.* **2005**, *7* (S2), 1991.
- (74) Harris, R. K.; Hodgkinson, P.; Picard, C. J.; Yates, J. R.; Zorin, V. Chemical Shift Computations on a Crystallographic Basis: Some Reflections and Comments. *Magn. Reson. Chem.* **2007**, *45*, S174–S186.
- (75) Esrafil, M. D. Intra- and Inter-molecular Interactions in Salicylic Acid-Theoretical Calculations of ^{17}O and ^1H Chemical Shielding Tensors and QTAIM Analysis. *Can. J. Chem.* **2011**, *89*, 1410–1418.
- (76) Esrafil, M. D.; Alizadeh, V. A Theoretical Investigation of Hydrogen Bonding Effects on Oxygen and Hydrogen Chemical Shielding Tensors of Aspirin. *Struct. Chem.* **2011**, *22*, 1195–1203.
- (77) Esrafil, M. D.; Alizadeh, V. Characterization of Intermolecular Interactions in Crystalline Aspirin: A Computational NQR Study. *Int. J. Quantum Chem.* **2012**, *112*, 1392–1400.
- (78) Dracinsky, M.; Hodgkinson, P. A Molecular Dynamics Study of the Effects of Fast Molecular Motions on Solid-State NMR Parameters. *CrystEngComm* **2013**, DOI: 10.1039/C3CE40612A.